Electronic Supplementary Information

A dual emission metal-organic framework for rapid ratiometric fluorescence detection of CO_3^{2-} in seawater

Yu Wei,[a] and Yan Xia*[abcd]

[a]Research Center for Analytical Sciences, College of Chemistry, Nankai University, Tianjin 300071, China

[b]Key Laboratory of Biosensing and Molecular Recognition

[c]State Key Laboratory of Medicinal Chemical Biology (Nankai University)

[d]Collaborative Innovation Center of Chemical Science and Engineering (Tianjin)

Text S1

Linear equation is Y = 0.85386 - 0.00275 X and $R^2 = 0.9612$. The following equations evaluate the LOD of CO_3^{2-} detection system.

$$S_b = \sqrt{\frac{\sum(F_0 - F_1)}{N-1}} = 8.78 \times 10^{-3}$$

$$LOD = 3S_b / S = 9.58\ \mu M$$

Where S_b is the standard deviation for replicating detections of blank solutions (N = 20); F_0 is the fluorescence intensity of IRMOF-10-Eu in water; F_1 is the average of F_0; and S is the slope of the linear relationship in Fig. 4B ($S = 2.75 \times 10^3\ M^{-1}$).

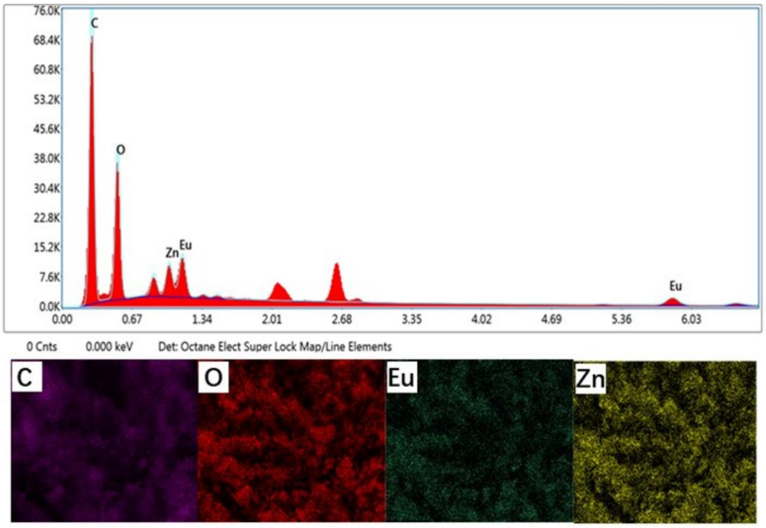

Fig. S1 SEM elemental mapping of IRMOF-10-Eu.

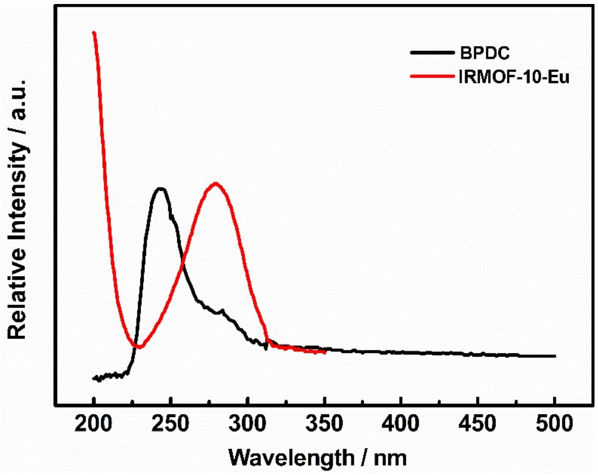

Fig. S2 UV-vis spectra of BPDC and IRMOF-10-Eu aqueous solutions.

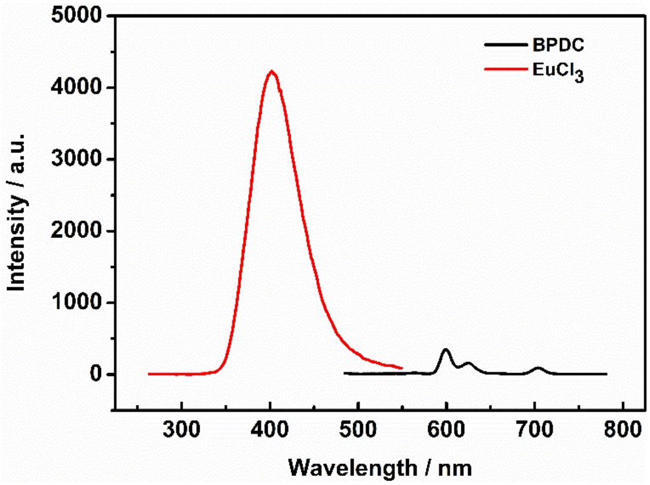

Fig. S3 Fluorescence spectra of BPDC (λ_{ex} = 250 nm) with the concentration of 0.05 mg mL^{-1} and EuCl$_3$ at the concentration of 10 mg mL^{-1} (λ_{ex} = 395 nm).

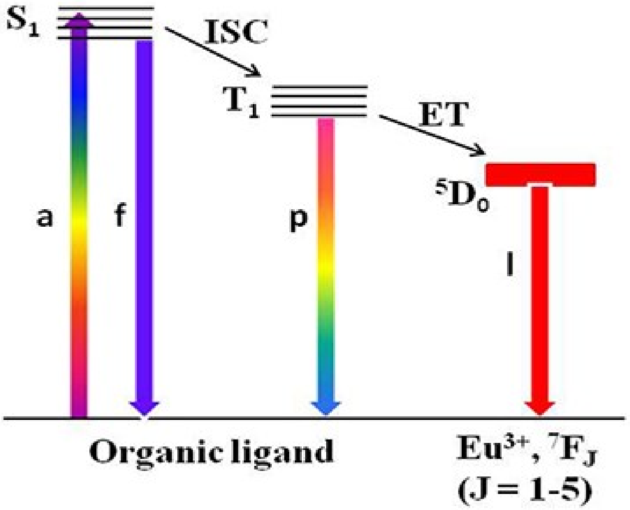

Fig. S4 Schematic representation of absorption, migration, and emission of IRMOF-10-Eu depicting with the antenna effect. [Abbreviations: "a"= absorption at 278 nm;"f"=fluorescence at 365 nm;"p"= phosphorescence;"l"= luminescence around 580-710 nm from Eu^{3+} in IRMOF-10-Eu. ISC = intersystem crossing; ET = energy transfer; S = single; and T = triplet.]

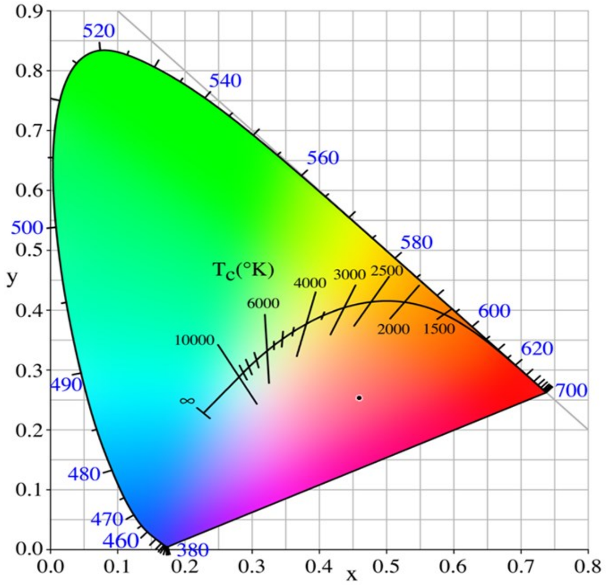

Fig. S5 The corresponding CIE chromaticity of IRMOF-10-Eu.

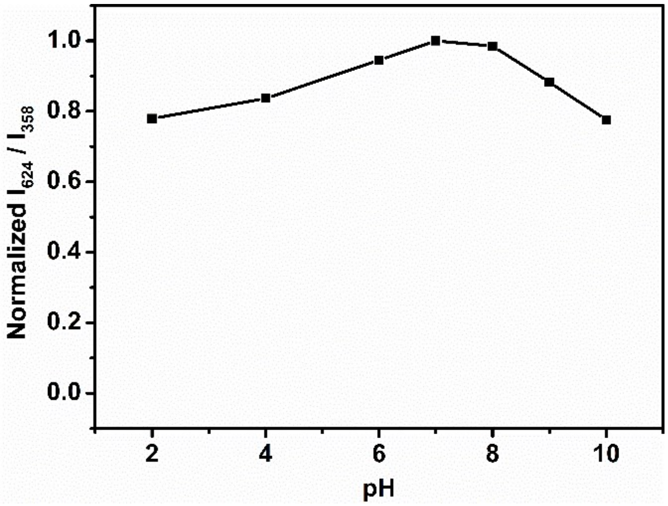

Fig. S6 Effect of pH on the fluorescence intensity of IRMOF-10-Eu (0.05 mg mL^{-1}) under excitation at 278 nm.

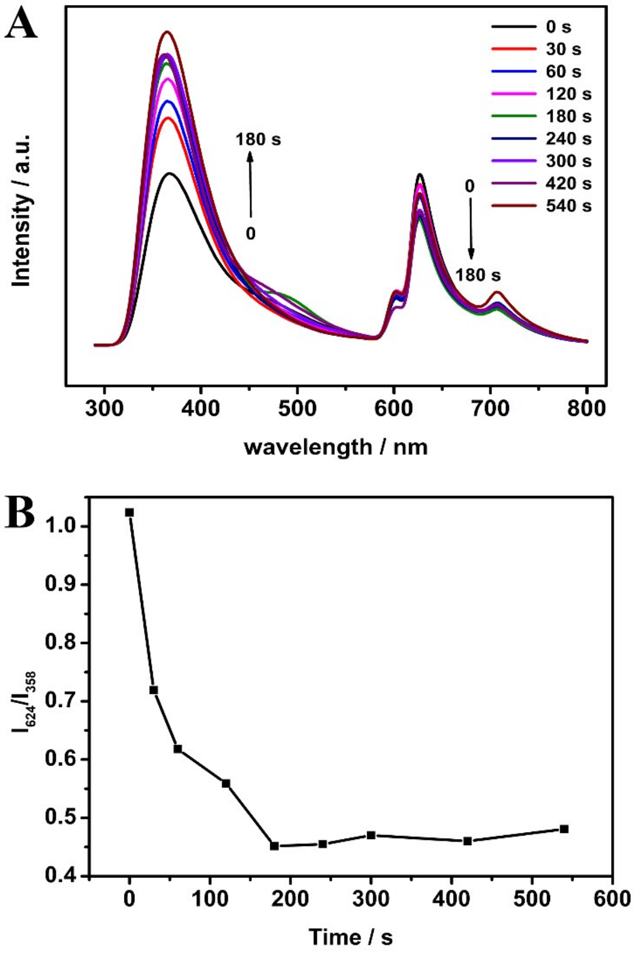

Fig. S7 (A) Fluorescence spectra of the IRMOF-10-Eu in 100 μM CO_3^{2-} solution with different reaction time; (B) Plot of the intensity ratio of I_{624}/I_{358} versus time.

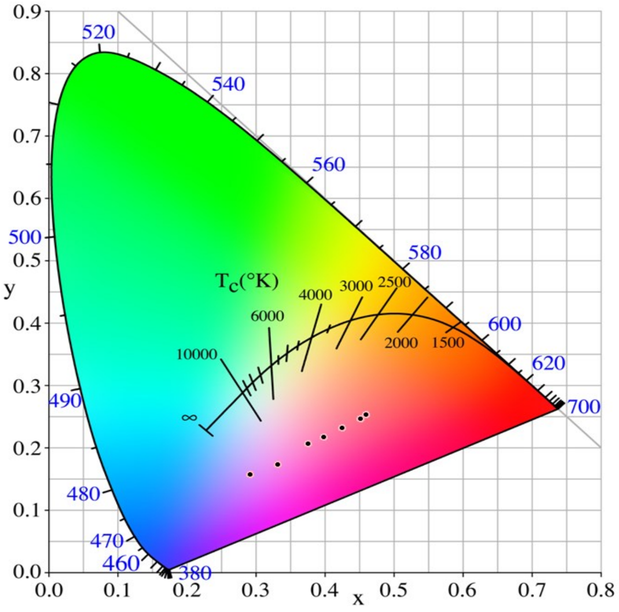

Fig. S8 The corresponding CIE chromaticity of IRMOF-10-Eu in the presence and absence of CO_3^{2-} (0-500 μM).

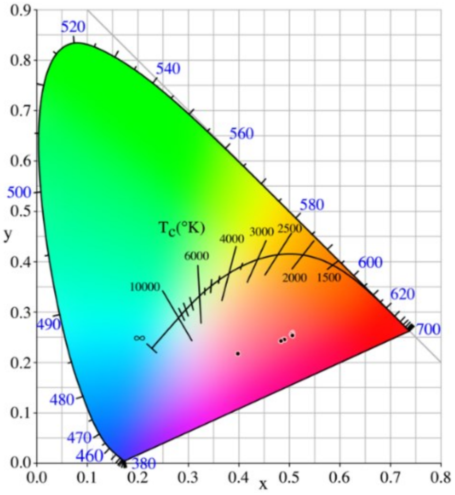

Fig. S9 The corresponding CIE chromaticity of IRMOF-10-Eu after addition of different ions (300 μM CO_3^{2-}， 500 μM other interference ions).

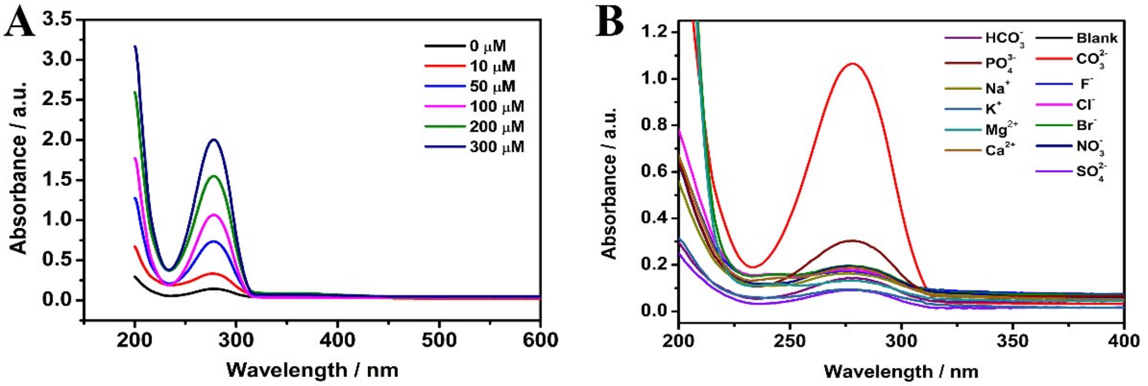

Fig. S10 (A) UV-vis spectra of IRMOF-10-Eu before and after addition of CO_3^{2-}; (B) UV-vis spectra of IRMOF-10-Eu after addition of various anions.

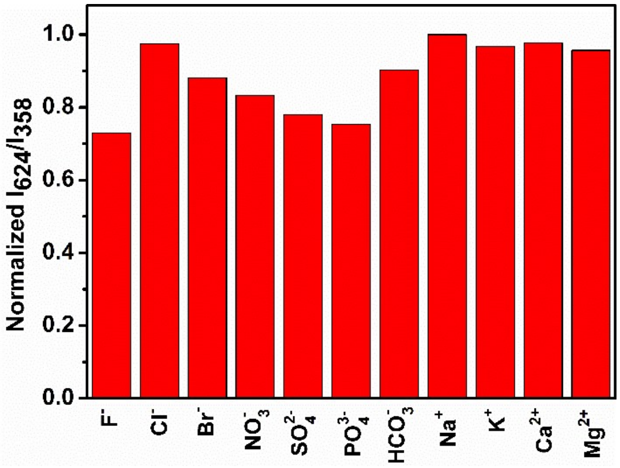

Fig. S11 Normalized I_{624}/I_{358} intensity ratio in the presence of the other ions (300 μM CO_3^{2-} + 500 μM interference ions) to illustrate their interference on the determination of carbonate ions.

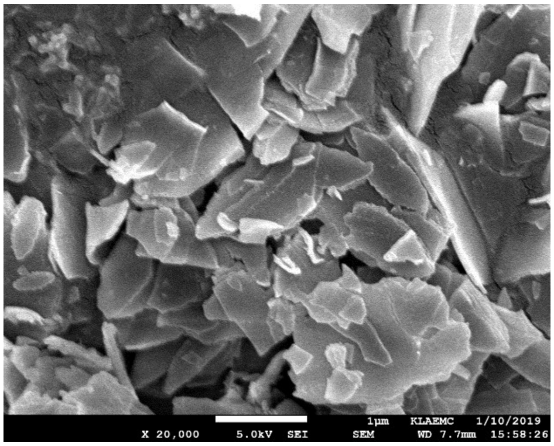

Fig. S12 The SEM of IRMOF-10-Eu after added 500 μM CO_3^{2-} ions.

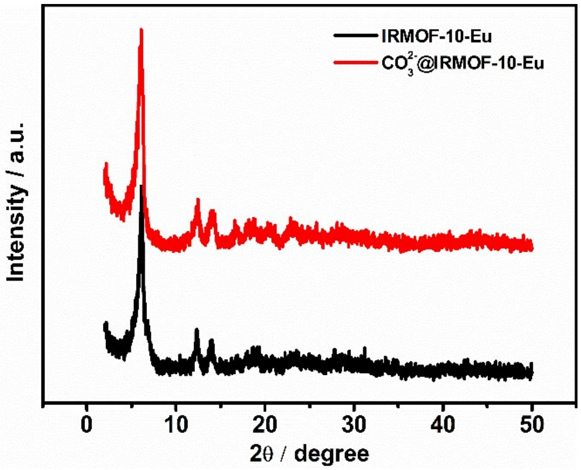

Fig. S13 XRD pattern of the synthesized IRMOF-10-Eu before and after the interaction with 500 μM CO_3^{2-}.

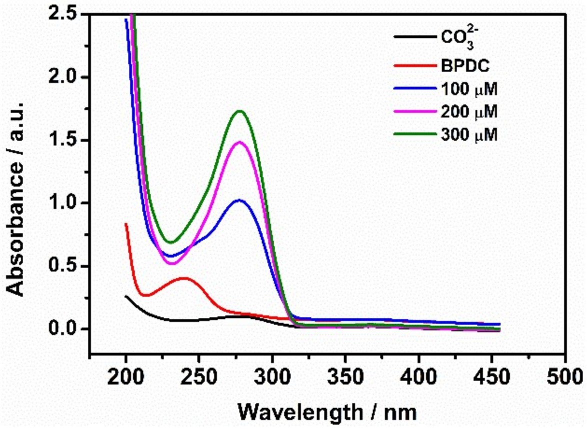

Fig. S14 UV-vis spectra of BPDC before and after the interaction with CO_3^{2-}

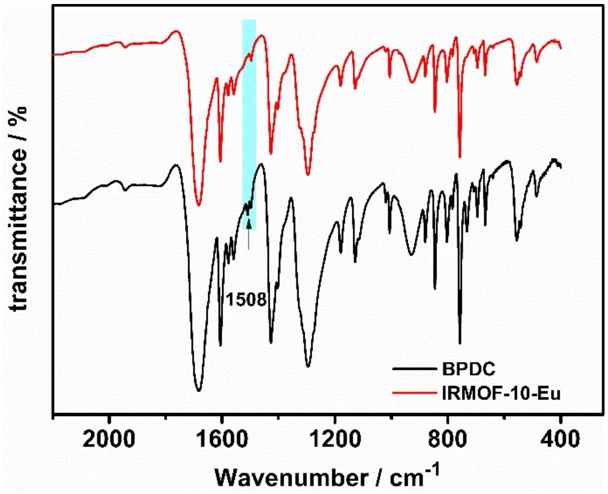

Fig. S15 FT-IR spectra of BPDC before and after the addition of CO_3^{2-} (300 μM)

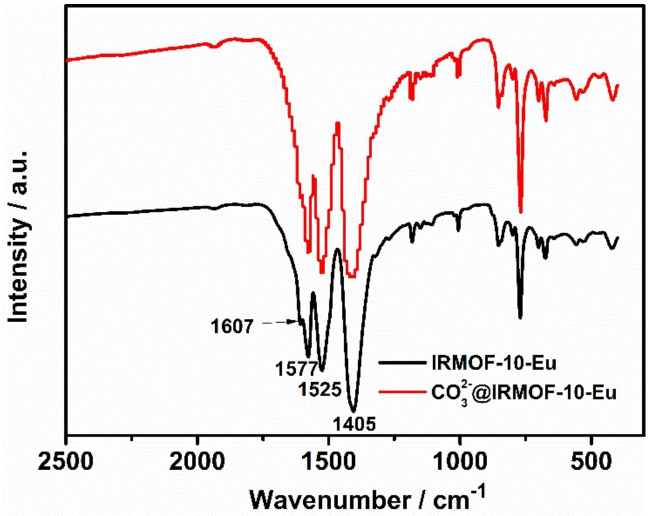

Fig. S16 FT-IR spectra of IRMOF-10-Eu before and after the addition of CO_3^{2-} (300 μM)

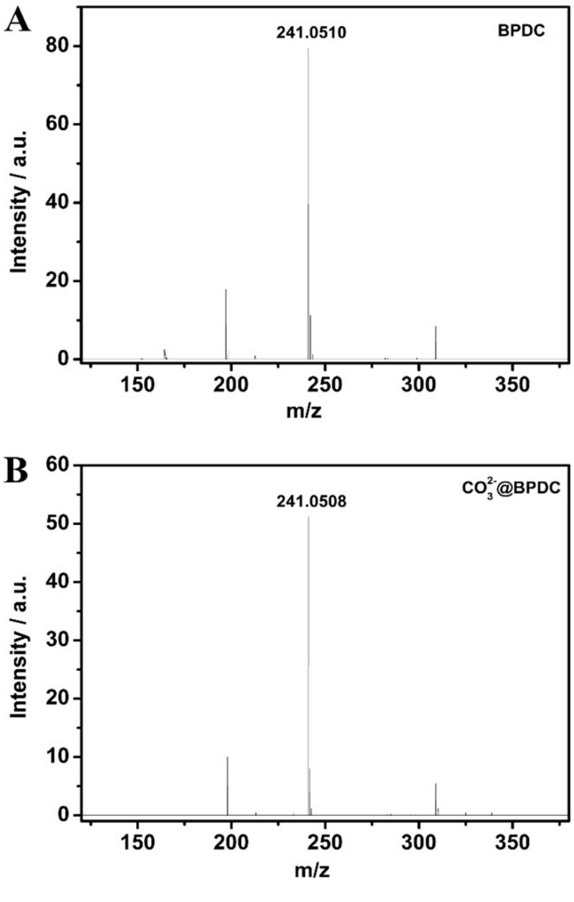

Fig. S17 Mass spectra of BPDC in DMSO before and after the addition of CO_3^{2-} (300 μM).

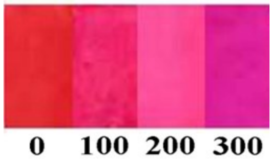

Fig. S18 Photographs showing ratiometric fluorescence color change of the IRMOF-10-Eu test strip response to different carbonate ions（0-300 μM）.

Table S1 Comparison of low detection limit of various materials for CO_3^{2-}.

sensor	LOD/μM	Reference
IRMOF-10-Eu	9.58	this work
PDZ-1	110	1
bis-urea calix[4]arene 1	120	2
$[Eu_2(pip)_2(OAc)_6]^a$	11.2	3
$[Eu(H_2O)_2(DO3A)]^b$	400	4

[a] pip denoted monotopic 2-phenylimidazo[4,5-f][1,10]phenanthroline; [b] H_3DO3A denoted 1,4,7,10-tetraazacyclododecane-1,4,7-triacetic acid.

Table S2 ICP-OES analysis of the solution after immersed IRMOF-10-Eu for 24 h.

Concentration of CO_3^{2-} (μM)	0	100	300	500
Concentration of Eu^{3+} (μg/ml)	2.81	256	266	371

Table S3 Main components of seawater.

Sea area	Concentration（mg/mL）									
	Na^+	Ca^{2+}	K^+	Mg^{2+}	Sr^{2+}	Cl^-	Br^-	NO_3^-	PO_4^{3-}	SO_4^{2-}
Wenchanghai	57.4	3.94	1.24	3.86	0.0080	25.9	2.19	1.52	0.183	3.09
Yellow Sea	43.4	3.01	1.21	3.42	0.0077	23.5	1.99	1.59	0.101	2.73
Yinggehai	58.8	4.42	1.23	4.00	0.0080	22.5	1.13	1.96	0.540	2.97
Beibu Gulf	56.4	3.88	1.40	3.77	0.0078	23.7	1.89	1.52	0.091	2.85

References

[1] THIMARADKA V, PANGANNAYA S, MOHAN M, et al. Hydrazinylpyridine based highly selective optical sensor for aqueous source of carbonate ions: Electrochemical and DFT studies[J]. Spectrochimica Acta Part A: Molecular and Biomolecular Spectroscopy, 2018, 193: 330-337.

[2] LEE H K, OH H, NAM K C, et al. Urea-functionalized calix[4]arenes as carriers for carbonate-selective electrodes[J]. Sensors and Actuators B: Chemical, 2005, 106(1): 207-211.

[3] LU Y N, PENG J L, ZHOU X, et al. Rapid naked-eye luminescence detection of carbonate ion through acetonitrile hydrolysis induced europium complexes[J]. CrystEngComm, 2018,

20(46): 7574-7581.

[4] VANEK J, LUBAL P, HERMANN P, et al. Luminescent Sensor for Carbonate Ion Based on Lanthanide(III) Complexes of 1,4,7,10-Tetraazacyclododecane-1,4,7-Triacetic Acid (DO3A)[J]. Journal of Fluorescence, 2013, 23(1): 57-69.